

Advanced VUV Spectrometer for F₂ Laser Metrology
Eckehard Onkels, German Rylov, Richard Sandstrom

Cymer, Inc., San Diego, CA 92127

ABSTRACT

The advent of 157 nm F₂ lasers in lithographic application implied new challenges in spectral metrology. The approaches for the lithographic imaging system, that have been suggested so far, differ in the requirements of the spectral bandwidth of the laser. However, even designs with less stringent demands will require high-resolution spectral metrology in order to enable comprehensible spectral bandwidth and purity measurements or specifications.

Ideally, narrowband calibration sources in the VUV range should be used to precisely determine the instrument function of the spectrometer, enabling correct spectral de-convolution. However, most schemes for generation of appropriate light sources are rather complex and thus expensive. Stability and lifetime of solid state sources, i.e. nonlinear optical devices, are expected to be not satisfying too.

The principal approach for a spectrometer design should be to increase the inherent spectral resolution of the instrument above the required specification limits of the laser systems under investigation, avoiding or at least significantly reducing the necessity of spectral de-convolution.

Following this path, the optical layout of an existing Echelle grating based spectrometer has been investigated and re-designed. Collimation and imaging quality of the spectrometer could be considerably improved with the implementation of an aspheric focussing mirror.

Keywords: VUV Metrology, High-resolution spectroscopy, Lithography, F₂ laser

1. GENERAL DESIGN CONSIDERATIONS

Aside highest possible spectral resolution, several other performance characteristics have to be kept in mind during the design of a VUV spectrometer for use with narrowband lithography F₂ lasers. Among these were compactness, large dynamic range, low background (E95) and insensitivity to the red and infrared emission of F₂ lasers. The ability to pre-adjust the spectrometer beam path with visible light sources significantly reduces overall alignment and total built time. This can be achieved by an all-reflective beam path design. An echelle grating based spectrometer design was chosen for its theoretically predicted resolution and off-the-shelf availability of appropriate optical elements. The achievable spectral resolution of echelle grating based spectrometers is not only limited by total size and imperfections of the grating, also, the imaging quality of the entire optical path is likewise important. At the short wavelengths of VUV radiation, surface contour and quality critically influence aberrations and scatter. Illumination of grating and separation of incident and exiting beam on the grating surface implies off-axis alignment of the focal mirror(s). Under this constraint, spherical mirrors demand largest practical focal lengths and lowest possible off-axis angles to minimize numerical aperture, NA, and correlated image errors. However, both requirements can be fulfilled only within reasonable limits given from overall size. Alternatively, aspheric focussing mirrors, i.e. off-axis parabolic mirrors, can be employed to significantly reduce imaging errors and focal lengths requirements, enabling a very compact design.

Obviously, the entire spectrometer has to be either purged with nitrogen or evacuated to circumvent the strong absorption from oxygen. Although the latter approach appears most consequent, it has several

drawbacks, mainly from practical considerations. Since the effect of pressure forces should be eliminated from the opto-mechanical setup to maintain precise optical alignment, which requires either very stiff enclosures designs (i.e. cast material) or a sub-frame design enclosed in a vacuum vessel. Aside the additional need of a vacuum pump system, both approaches significantly increase system weight, size and total volume, dis-improving handling. A careful designed purge system can avoid these constraints without impact on the performance.

Precise determination of the bandwidth containing 95% of the spectral energy, E95, turns low background level and rapid drop of the instrument slit function outside its FWHM range into a very important characteristic. Likewise, appropriate selection of detector and data acquisition system is stringent to achieve a large dynamic range of detection.

F₂ lasers may emit several lines in the visible and infrared range, which can seriously impact the background level of the spectrometer, as these wavelengths get reflected very well within the spectrometer unless absorptive coatings are applied. Unfortunately practically all of these materials will deteriorate or/and outgas under exposure of VUV radiation, which should be strictly avoided to maintain detection sensitivity over extended periods. Choosing solar-blind detectors entirely avoids these difficulties.

2. EXPERIMENTAL SETUP

The entire setup fits on an optical table of 1 ft x 3 ft size. A custom made metal enclosure of 1 ft height seals the spectrometer. Several ports for nitrogen are provided to purge the volume. Care has been taken for the location of the purge inlets to ensure sufficient purge flow with minimal generation of turbulence which could affect optical performance due to creation of density related optical Schlieren effects, i.e. within the area of the collimated beam in front of the grating. An external oxygen sensor is used to control and monitor the purge gas quality. Typical readings are less than 3 ppm of oxygen at nitrogen flow rates of 2-3 std l/min.

The optical input port employs a KF-40 vacuum flange with an additional isolation CaF₂ window protecting the internal volume from potential contamination and pressure changes from exterior beam delivery systems. An echelle grating of 10'' length with a dispersion of about 60 mrad/pm at 157 nm is used for spectral separation. The internal beam path is folded to further increase the compactness of the design. Both of the designs investigated, spherical and aspherical focal mirror, use a 1m primary focal length with the focal mirror being used both for grating incident and exiting beam. Several mechanical feedthroughs allow fine adjustments of slit positions and grating angle during purged operation. In case of the off-axis parabolic mirror design an additional off-axis alignment has been provided. Spectral data is measured in a scanning slit mode, provided by a fast and solar-blind photomultiplier assembly mounted on a stepper motor actuated linear stage. An external Labview based system handles stepper motor control and acquisition of data. The signal sampling and acquisition routine can be synchronized with the pulsed laser source, various data handling routines provide online processing and display of spectral data and acquisition system status.

3. PERFORMANCE EVALUATION

In a first approach a 1 m spherical focal mirror has been implemented. The off-axis angle has been minimized to about 3 degree, which was the practical limit given from mounting space and free aperture. Initial scans during pre-alignment with a 632.8 nm He-Ne laser light source clearly showed slit-image

distortions due to aberrations of the focal mirror, as shown in Fig. 1 for various apertures in front of the focal mirror. During the instrument slit function measurements the grating had been replaced by a $\lambda/40$ reference flat.

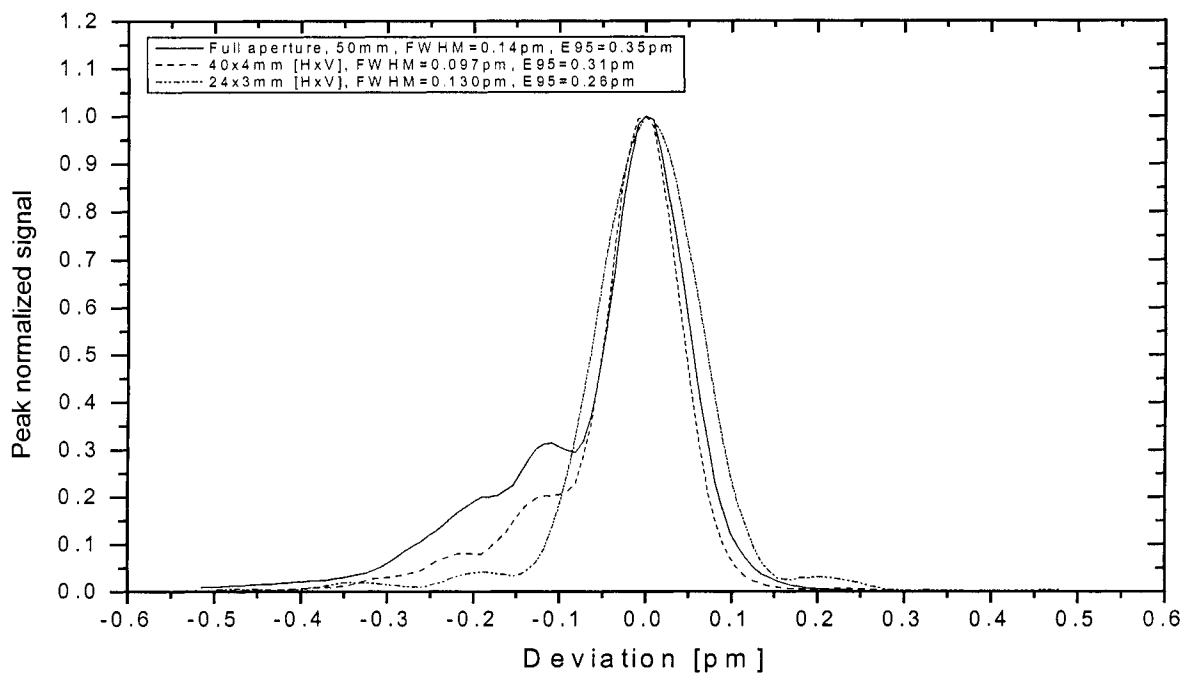


Figure 1: Instrument slit function at 623.8 nm, spherical focus mirror, hor. scale s. text

The scale factor of the horizontal axis has been adapted to the grating dispersion at the target wavelength to reflect a nominal 157 nm wavelength for interpretation of the inherent limits on spectral resolution. However, the image errors at this wavelength are almost certainly worse than shown here. Obviously, the aperture has to be significantly reduced to avoid severe slit image errors, i.e. on the left side of the instrument slit function. Unfortunately, this will not allow to exploit the full grating resolution. A reasonable criterium to choose the aperture would be for lowest E95, which, in the example given would be about 0.26 pm, at which point the FWHM of the instrument function already slightly increases to about 0.13 pm, still assuming direct transferability of 632.8 nm data to 157 nm .

Since these results were not satisfying, the spectrometer has been re-designed to allow the use of an aspheric focussing mirror, namely an off-axis parabolic mirror (OAP), which should significantly reduce spherical aberration. Fig. 2 shows a comparison of instrument slit functions with this design and the previous measured at 632.8 nm with a reference flat replacing the grating, again with the horizontal scale adapted to a nominal 157 nm wavelength. It is worth noting that the OAP results were achieved without apertures.

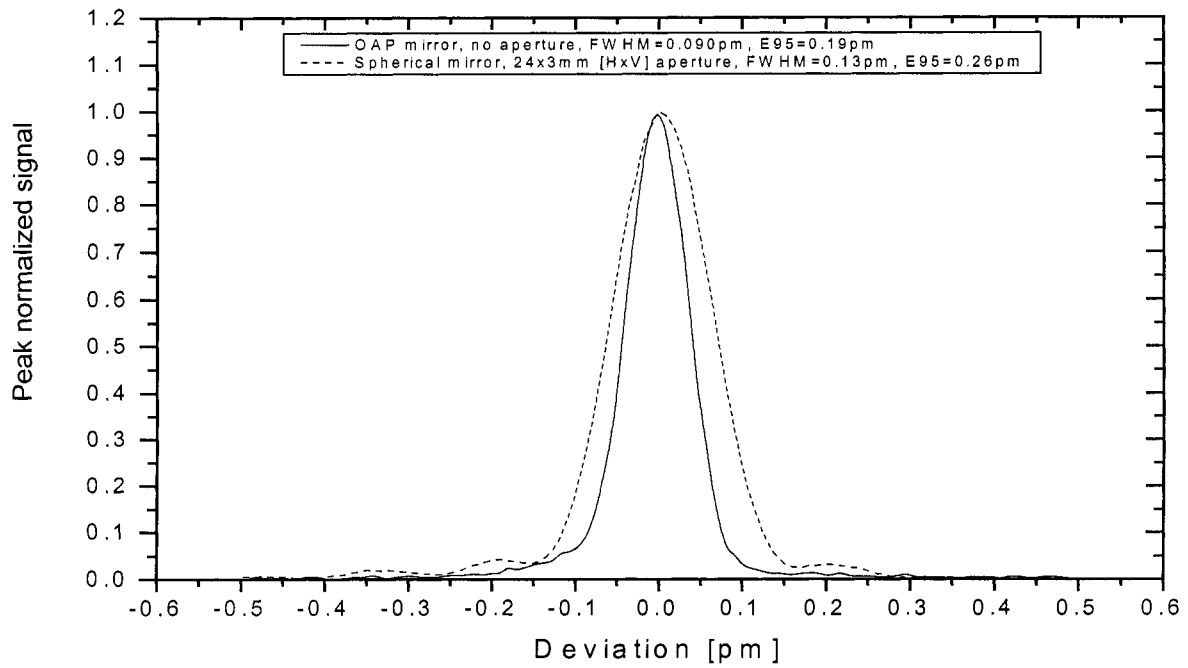


Figure 2: Slit functions obtained with OAP focus mirror and spherical mirror, 632.8 nm, hor. scale s. text

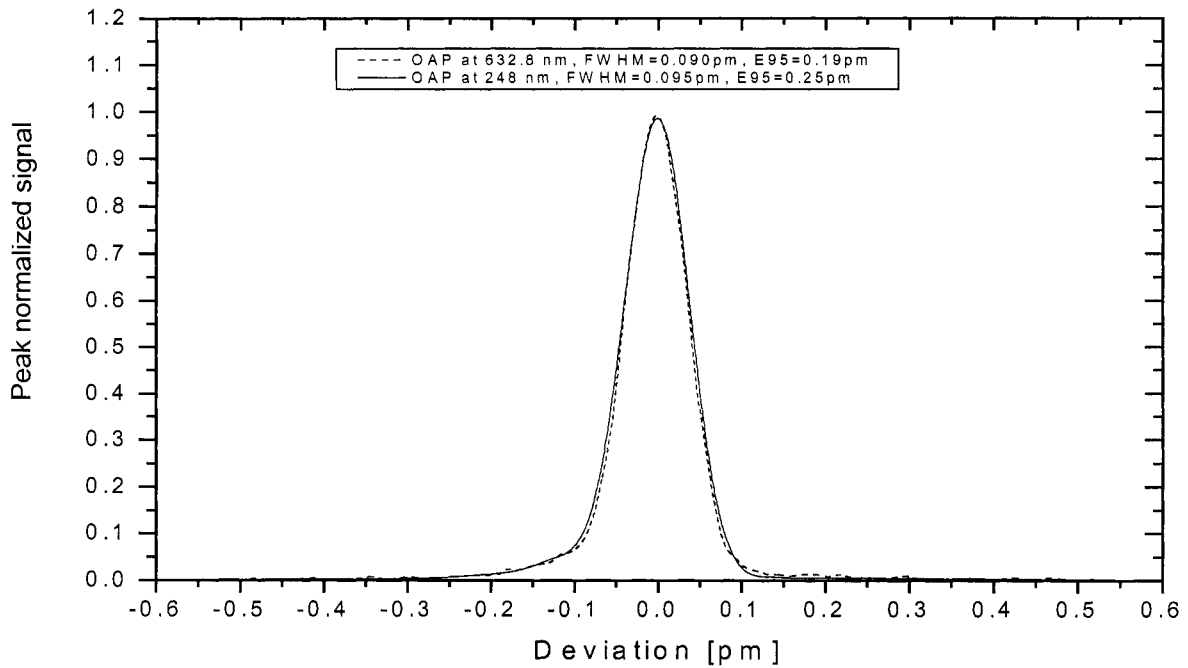


Figure 3: Comparison of instrument slit function measured at 632.8 nm and 248 nm, hor. scale s. text

Both FWHM and E95 resolution are significantly improved, to about 0.09 pm and 0.19 pm respectively *1). For the aspherical focus mirror design additional performance tests were carried out with a frequency-doubled Ar⁺ laser at 248 nm wavelength. Fig. 3 shows a comparison of the instrument slit function measured at 632.8 nm and 248 nm, with the wavelength scale modified as before. The increase in FWHM from 0.09 pm to 0.095 pm at the shorter wavelength is negligible, E95 marginally increases from 0.19 pm to 0.25 pm.

Fig. 4 shows the results of scans with the grating inserted and with the grating replaced by a reference flat. As in the examples shown above, the horizontal scale factor has been adapted to a nominal 157 nm wavelength.

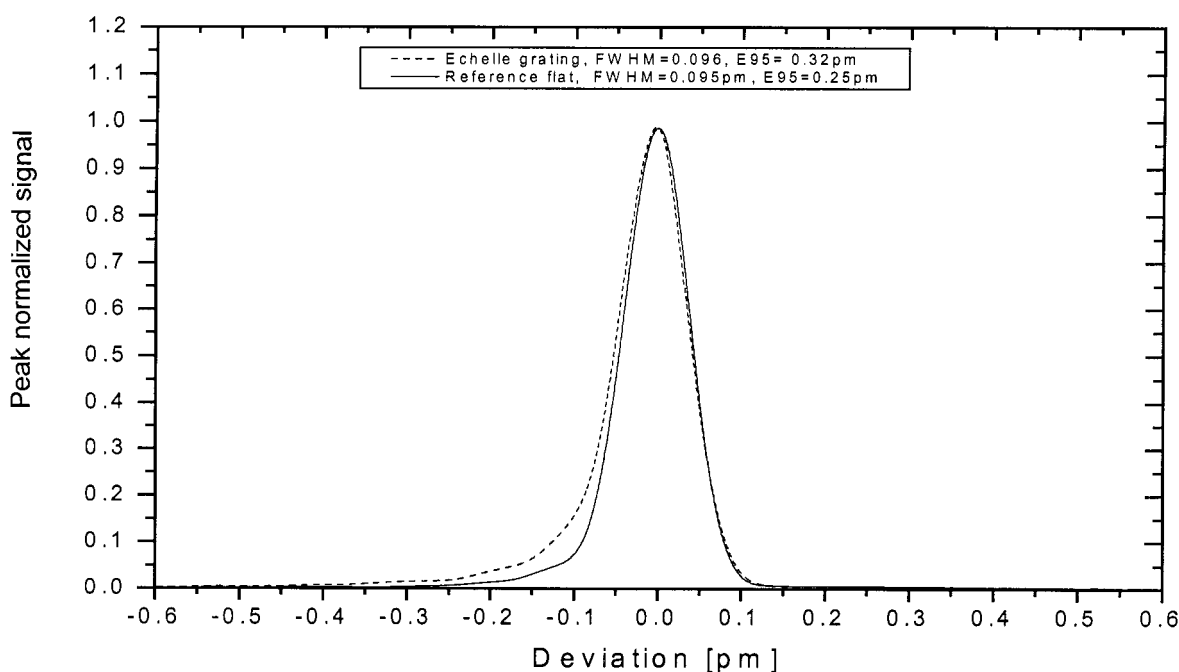


Figure 4: OAP instrument slit function at 248 nm with grating and reference flat, hor. scale s. text

The resolution limit imposed from the imaging optics is about 0.095 pm FWHM, and 0.25 pm E95 at the target wavelength 157 nm. With the grating in place, FWHM increases only marginally, E95 increases to about 0.32 pm. The observed broadening might be attributed to imperfections of the grating, i.e. surface figure and ghost images. Comparison of the FWHM and E95 values determined at 248 nm with the corresponding values at 632.8 nm shows very good agreement for the FWHM, however, the E95 values differ considerably. The increase at shorter wavelength indicates the presence of residual aberrations in the system with a significant contribution of the grating.

*1) The scan range extends far beyond the range shown here to ensure the inclusion of essentially the entire spectral energy, which is critical for precise determination of associated E95 values.

Results of theoretical calculations on the spectrometers slit functions together with the 157 nm re-scaled slit function as measured at 248 nm are shown in Fig. 5. Assuming 40 mm aperture for the collimated beam in the spectrometer, the theoretical resolution can be determined to 0.0942 pm FWHM and 0.156 pm for E95. Both data sets agree very well, minor deviations can be related to small errors in the assumption of slit sizes and effective free aperture as well as aberrations of the spectrometer optics as discussed already.

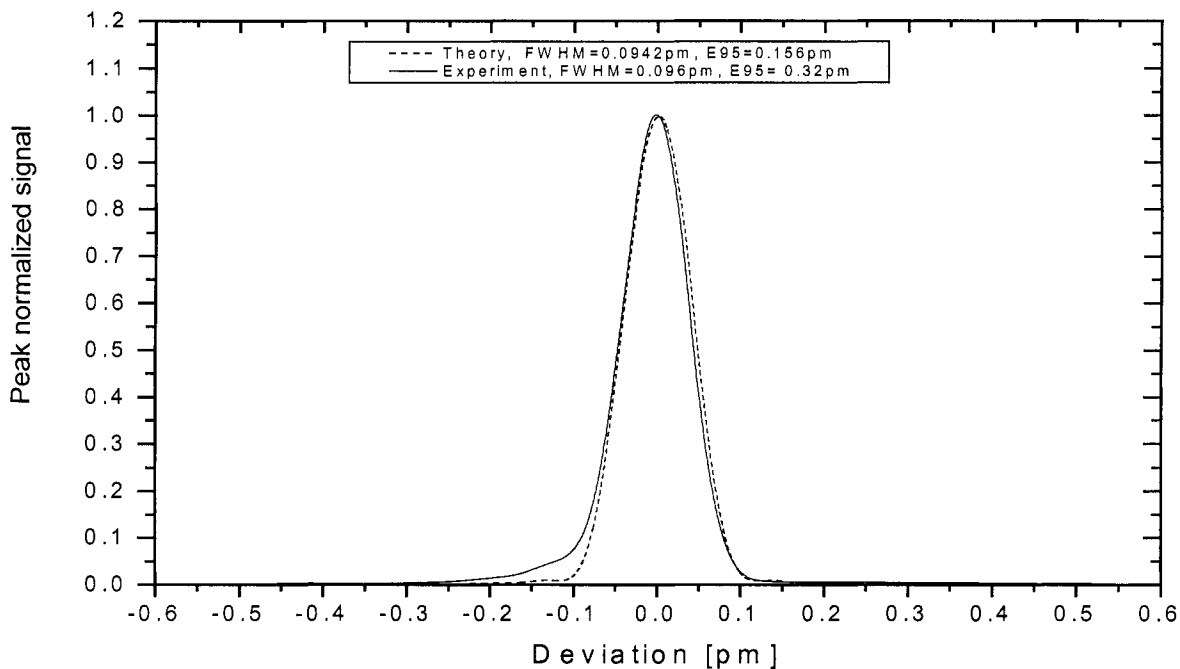


Figure 5: Comparison of theoretical and experimental instrument slit function, experimental data re-scaled to 157nm wavelength (s. text)

The spectrometer has also been used for parametric studies of F₂ laser operation to determine the effect of various parameters on bandwidth characteristics. Under assumption of diffraction limited performance of the spectrometer imaging optics, measured spectral data were forward convolved with the ideal slit function. In this manner an upper limit of the real source-emitted FWHM and E95 bandwidth can be evaluated, as the contribution of the spectrometer to broadening of measured spectra will be assumed minimal. Fig. 6 shows the result of this procedure for an experimental data set. The FWHM increases marginally from 0.598 pm to 0.608 pm upon forward convolution, the difference is practically below experimental repeatability. Similar, E95 remains almost unchanged with a small increase from 1.24 pm to 1.27 pm.

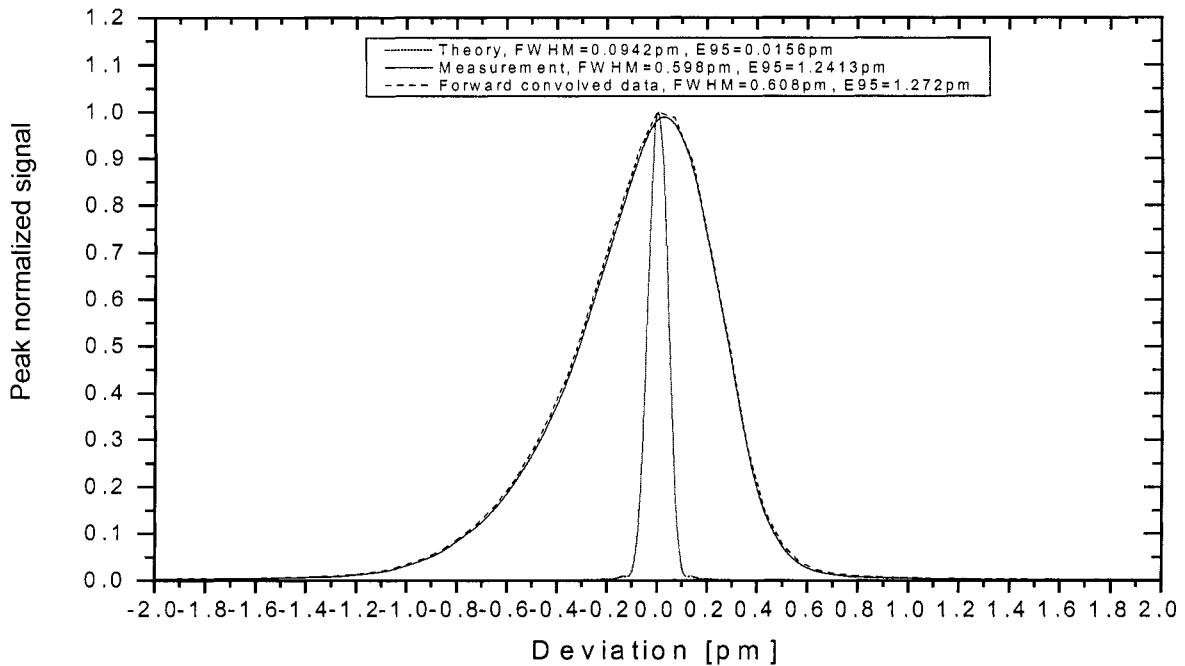


Figure 6: Experimental F_2 laser spectrum, theoretical instrument slit function and forward-convolved data set

4. PARAMETRIC STUDY OF F_2 LASER OPERATION

Comprehensive parametric studies on the performance of F_2 lasers, i.e. with respect to spectral characteristics, have been carried out to determine reasonable operating ranges for lithographic application. “Natural” bandwidth and wavelength centroid of F_2 lasers depend on various parameters, however, pressure induced changes are dominant /1,2/.

Fig. 7 and Fig. 8 show FWHM and E95 respectively obtained at various fill pressures. The partial pressure of F_2 remained constant at 0.5 kPa. Additional parameter is the applied charging voltage.

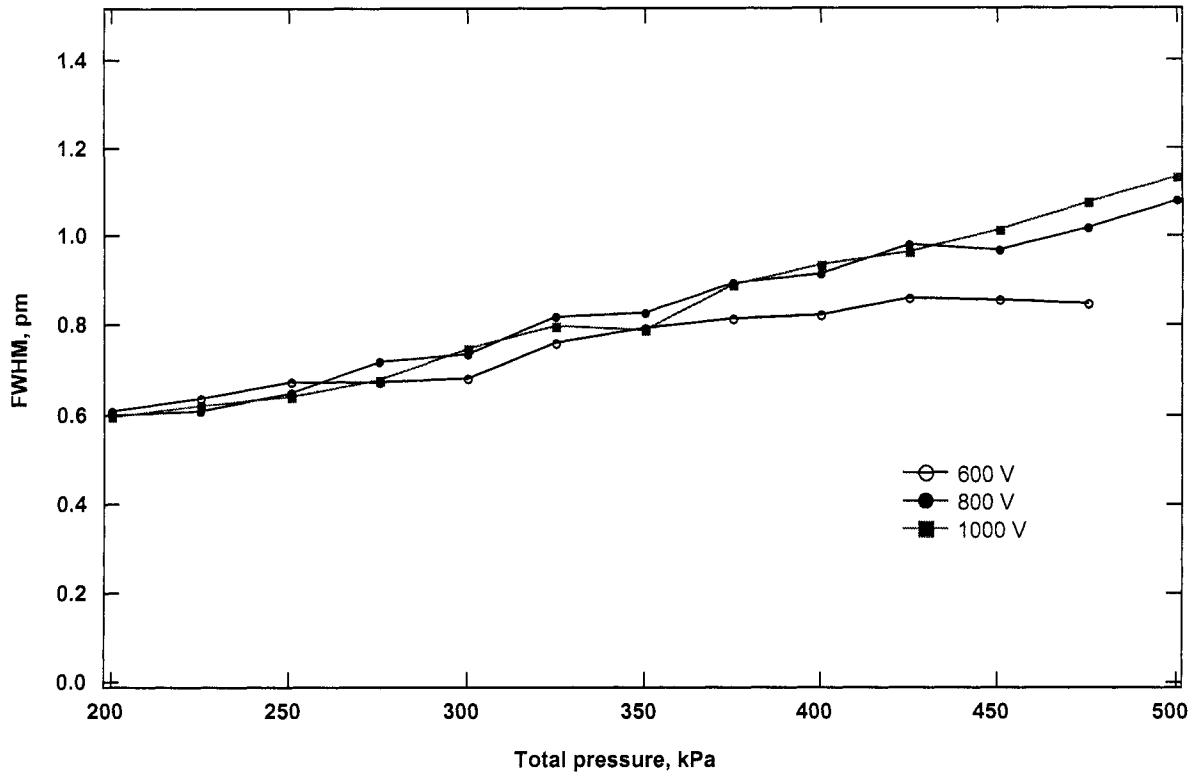


Figure 7: FWHM bandwidth vs. total fill pressure, 0.5 kPa F_2

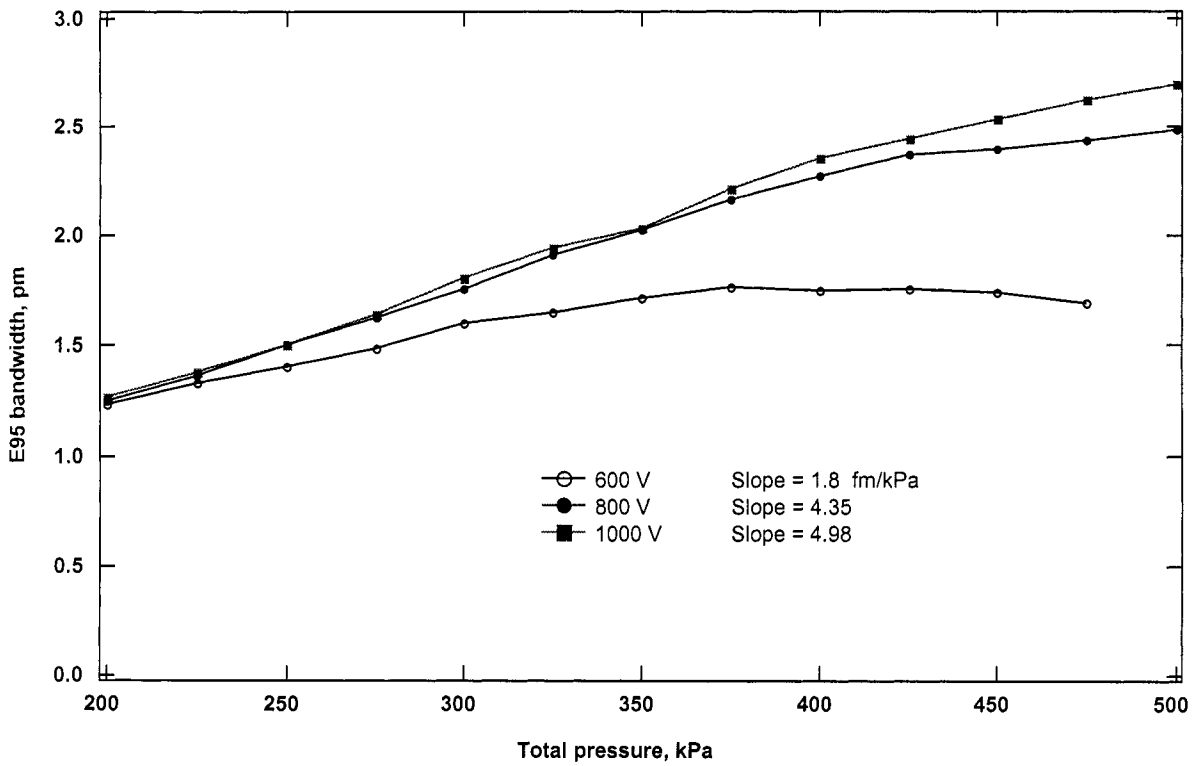


Figure 8: E95 bandwidth vs. total fill pressure, 0.5 kPa F_2

Within the range of parameters shown, the differential increase in FWHM and E95 broadening is roughly 1-2 fm/kPa and 2-5 fm/kPa respectively. The ratio between E95 and FWHM bandwidth is about 2-2.5. The emission spectrum of F₂ lasers is slightly asymmetric, with a tail towards the shorter wavelengths. A possible characterization can be given by an asymmetry function A(Δλ):

$$A(\Delta\lambda) := \frac{\int_{\lambda_0}^{\lambda_0+\Delta\lambda} I(\lambda) \partial\lambda - \int_{\lambda_0-\Delta\lambda}^{\lambda_0} I(\lambda) \partial\lambda}{2 \int_0^{\infty} I(\lambda) \partial\lambda} \quad \text{with} \quad \lambda_0 := \frac{\int_0^{\infty} \lambda \cdot I(\lambda) \partial\lambda}{\int_0^{\infty} I(\lambda) \partial\lambda} \quad (\text{center of mass wavelength})$$

Asymmetry can be defined as the absolute maximum of this function for all Δλ:

$$\text{Asymmetry} := \max(|A(\Delta\lambda)|)$$

Fig. 9 and 10 show experimental spectra, taken at variable pressure at high and low fluorine concentrations. For comparison of the spectral shape factor, all spectra have been normalized with respect to peak amplitude and bandwidth (1 pm). The shape shows only minor variations with pressure, which is also reflected by the calculated asymmetry as shown in Fig. 11.

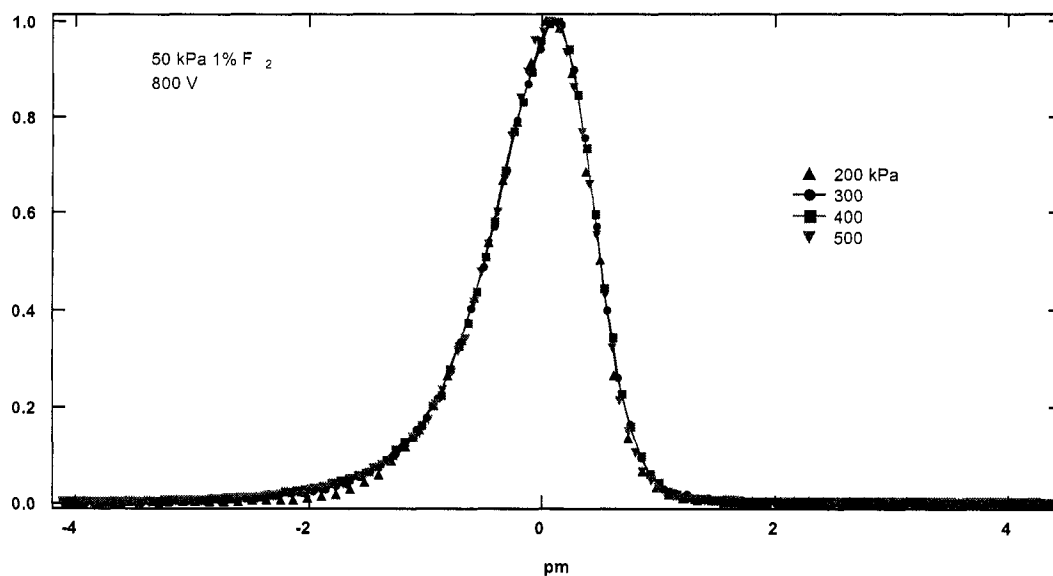


Figure 9: Spectral shape, normalized to 1pm FWHM bandwidth, at 0.5 kPa F₂

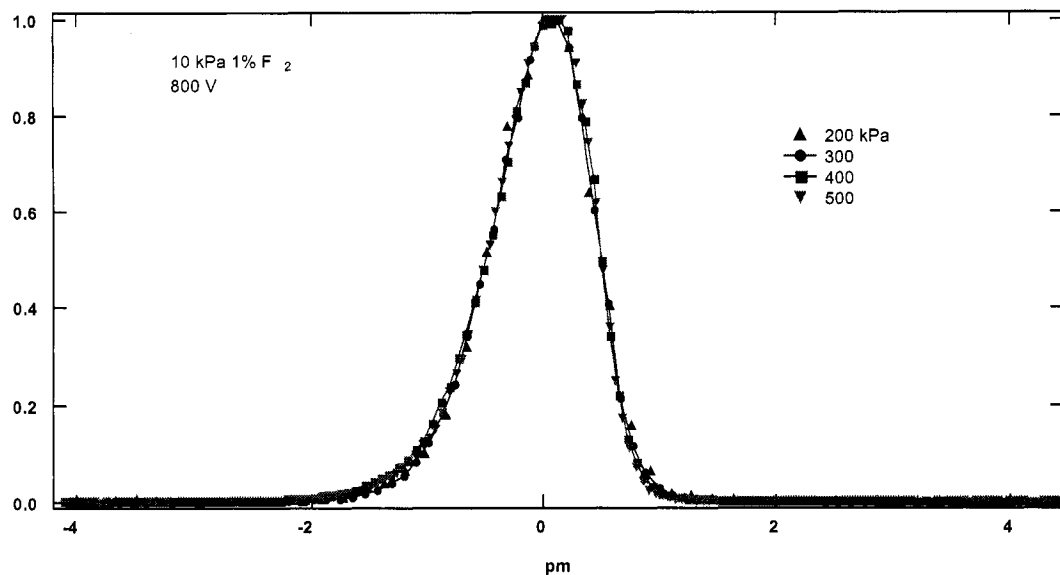


Figure 10: Spectral shape, normalized to 1 pm FWHM bandwidth, 0.1 kPa F₂

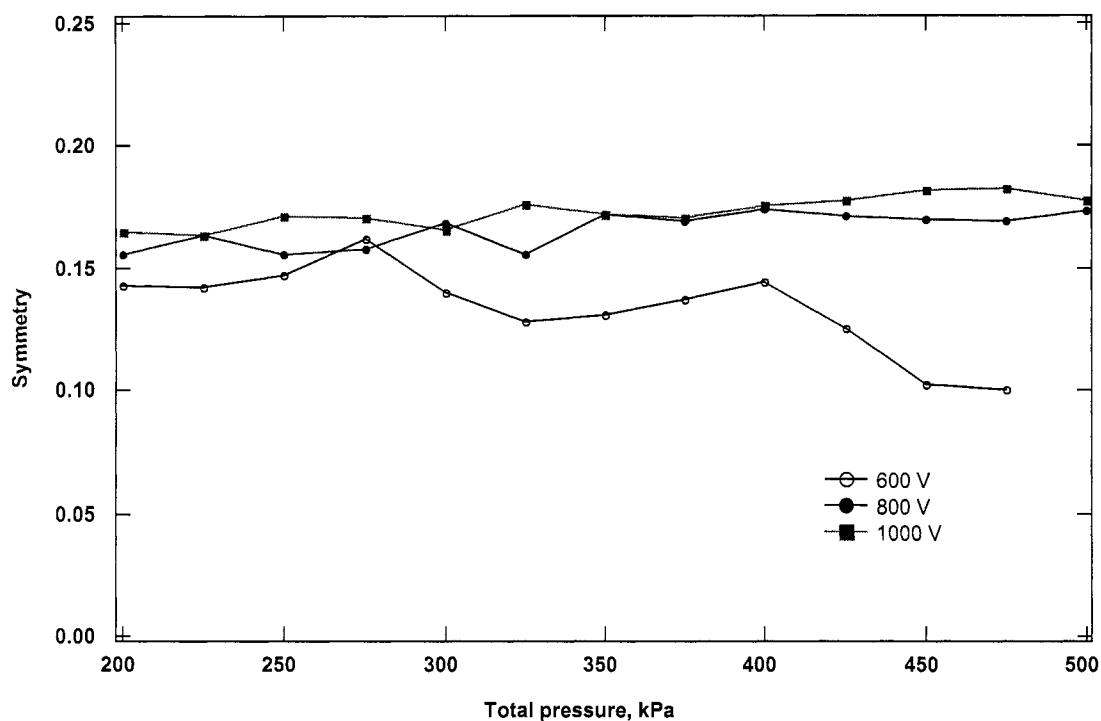


Figure 11: Asymmetry vs. total fill pressure, 0.5 kPa F₂

In addition to spectral data, energies in the VUV and red/IR have been measured to estimate efficiency and achievable energy levels with various operating parameters. Fig. 12 shows the total VUV energy vs. pressure at different voltage levels. At the lowest voltage, 600 V, discharge breakdown is hampered at higher total pressures.

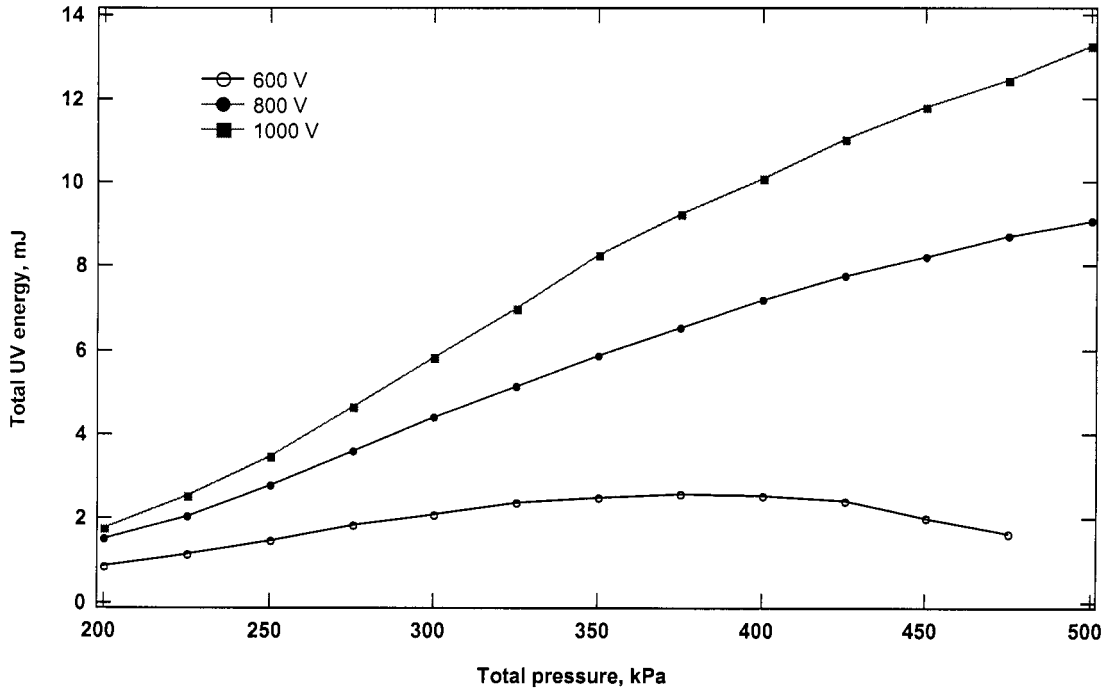


Figure 12: Total VUV energy vs. pressure, 0.5 kPa F₂

The reduction in efficiency at low pressure is partially due to premature breakdown of the discharge before the entire stored energy is transferred to the discharge capacitor assembly. Since the laser was operating with a broadband resonator design, both known VUV lines were emitted simultaneously. Fig. 13 shows the contribution of each line to the total output energy vs. pressure.

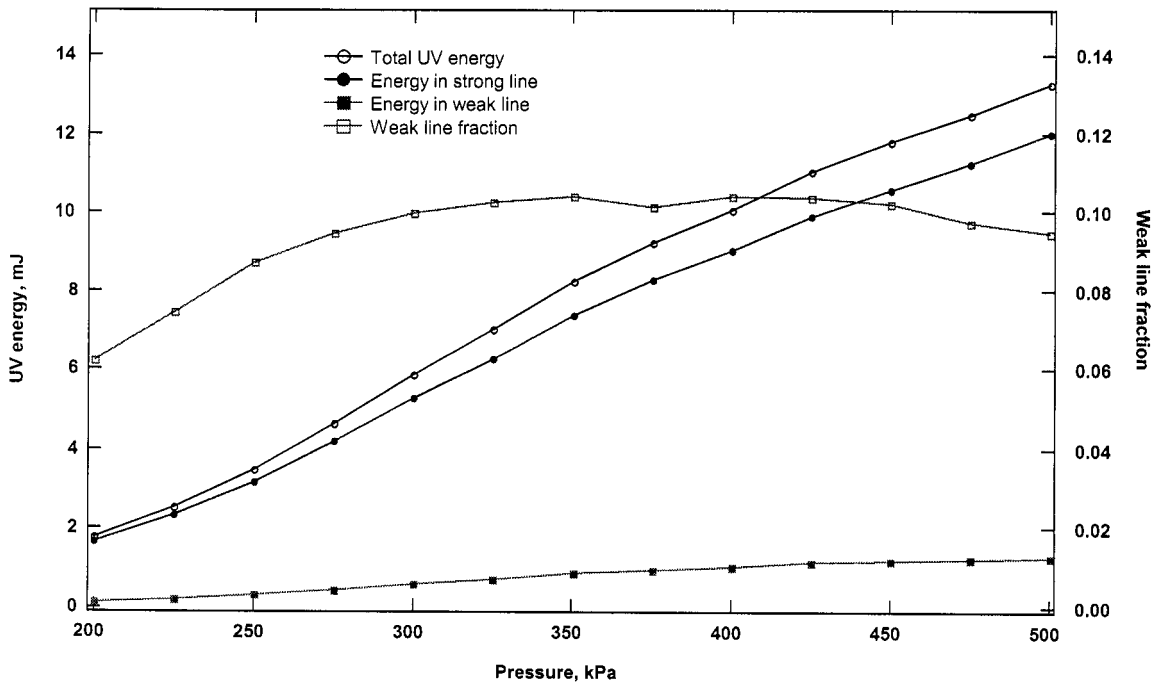


Figure 13: Strong line and weak line vs. pressure, 0.5 kPa F₂

The weak line contributes between 6% and 10% to the total output in the VUV range. Additional red and infrared emission occurs in super-fluorescent mode, with a slight increase towards lower pressures. Fig. 14 shows the fraction of red/IR energies to total UV power vs. pressure.

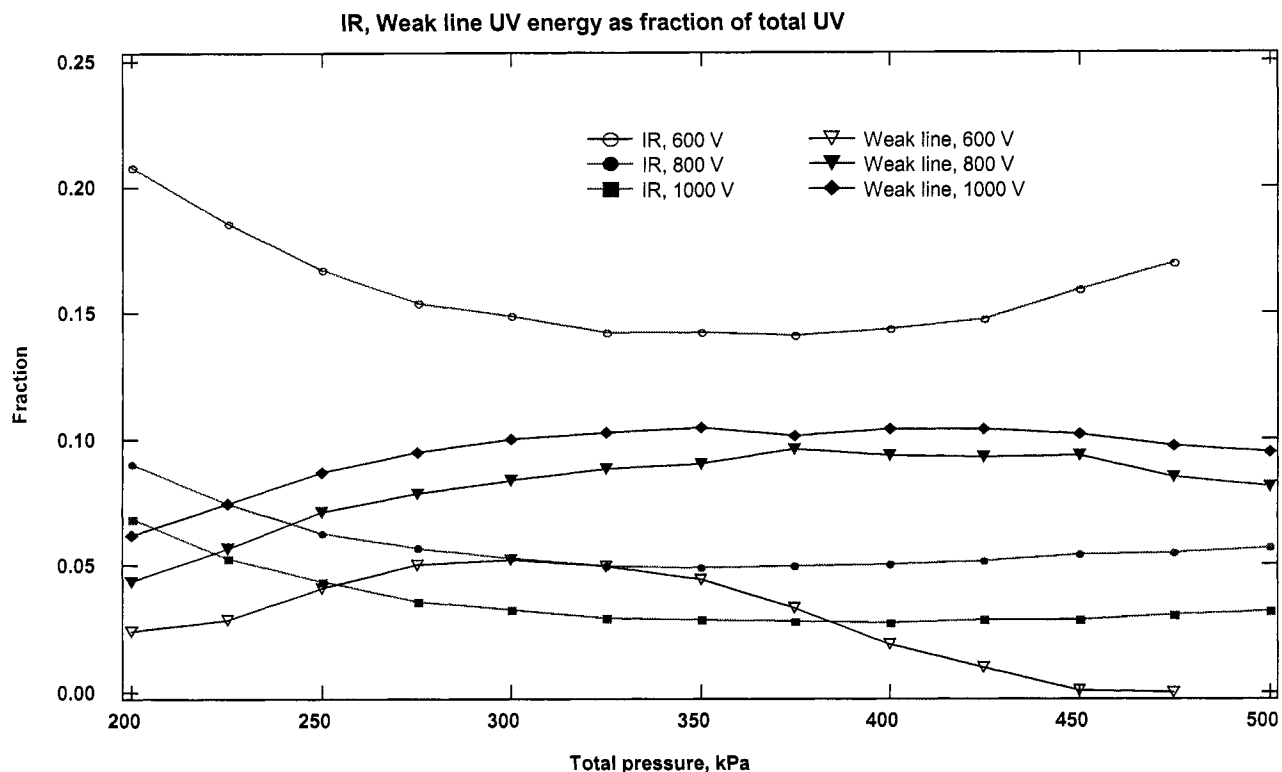


Figure 14: Red/IR line energies as fraction of total VUV, 0.5 kPa F₂

5. CONCLUSION

Careful re-design of the optical layout and the implementation of an off-axis parabolic focus (OAP) mirror could significantly improve spectral resolution of an existing spectrometer for the VUV range. At these wavelengths aberrations become very strong even at relatively low numerical apertures (NA). Maintaining the principal spectral resolution power of the echelle grating implies the use of practically the entire surface, thus the maximum of available NA. For a previous design with a spherical mirror, the NA had to be reduced to ensure reasonable E95 bandwidth performance, however, at this point FWHM resolution increased already above acceptable values. Measurement and comparison of the instruments slit functions at various wavelengths of calibration light sources clearly demonstrate the superior imaging quality achieved with the OAP design. The majority of the remaining aberrations can be attributed to imperfections of the grating surface, i.e. planarity.

With the improved performance of the new spectrometer, comprehensive parametric studies on the performance of VUV F₂ lasers were carried out to investigate the influence of various parameters on spectral characteristics and output energies as well. FWHM and E95 bandwidth variations are dependent mainly on the total pressure within the laser discharge chamber. At the lower pressure limit of 200 kPa a FWHM of 0.6 pm can be achieved, however, with a significant reduction of laser efficiency.

6. REFERENCES

1. S. Nanzai, S. Nagai, J. Fujimoto, H. Mizoguchi, "Development of the line selected F2 laser G20F", SEMATECH 157nm Technical Data Review, (2000), San Diego, CA.
2. K. Vogler, I. Bragin, N. Niemoeller, F. Voss, E. Bergmann, I. Tassy, R. Paetzel, S. Gorvorkov, W. Walecki, "Reliable and field-proven F2 Lithography laser", SEMATECH 157nm Technical Data Review, (2000), San Diego, CA